



## Measurement of Lifetime Ratio for Neutral and Charged $B$ Mesons

The DØ Collaboration

URL: <http://www-d0.fnal.gov>

(Dated: March 29, 2004)

The measurement of the lifetime ratio for neutral and charged  $B$  mesons was performed using the statistics collected by DØ experiment in Run II and corresponding to approximately  $250 \text{ pb}^{-1}$ .  $B$  hadrons were reconstructed in semileptonic decays  $B \rightarrow \mu^+ \nu D^*(2010)^- X$ , which are dominated by  $B^0$  decays and  $B \rightarrow \mu^+ \nu D^0 X$ , which are dominated by  $B^+$  decays. The lifetime ratio was obtained from the variation of the ratio of events in these two processes at different decay lengths. The preliminary result is:

$$\tau^+/\tau^0 - 1 = 0.093 \pm 0.021 \pm 0.022$$

## I. INTRODUCTION

Study of heavy flavour lifetimes is intimately related with the understanding of decay dynamics of these particles. For instance, the much larger lifetime of the  $D^+$  compared to the  $D^0$  meson, while having equal semi-leptonic widths, implied that the non-leptonic decays of the former were being suppressed. This was explained by the destructive Pauli interference among the non-leptonic final states available to the  $D^+$ .

In recent years, inclusive decay rates of heavy hadrons have been calculated from first principles of QCD via a technique called Operator Product Expansion [1]. In this approach, leading non-perturbative corrections are at the order of  $1/m_Q^2$ , which is about 5% for B hadrons. Effects like Pauli Interference arise at  $1/m_Q^3$ , and the main effect is to cause lifetime differences between hadrons of the same flavour. Since the charm quark is light (compared to  $b$ ), these effects are rather large. For charm hadrons, OPE is only semi-quantitative, and the predictions roughly agree with data.

In the case of  $B$  hadrons, corrections are much smaller, and more precise predictions can be made. For instance, using inputs from quenched lattice QCD, NLO calculations [2] yield  $\tau^+/\tau^0 = 1.053 \pm 0.016 \pm 0.017$ . However, unquenching effects could be sizeable. In addition, OPE makes predictions for the lifetimes of other B hadrons, e.g.,  $\tau(\Lambda_b)/\tau(B_d^0) = 0.9 - 1.0$ ,  $\tau(B_s)/\tau(B_d)$  is approximately  $1.0 \pm \mathcal{O}(0.01)$ .

From the experimental point of view, the measurement of the ratio of lifetimes, rather than their absolute values, is more promising, since many systematic uncertainties cancel out. The DØ experiment is capable to observe all  $B$  hadrons simultaneously and to measure their lifetime in the same experimental environment, which further reduces the systematics. Combined with the large statistics of different  $B$  hadron decays, collected by DØ in Run II, the precise result on lifetime difference can be expected.

This note presents the measurement of the lifetime ratio of neutral and charged  $B$  mesons. After introducing in section II-IV the experimental method, the detector elements essential for this study, the event selection and simulation samples used, the sections V-VII give the detailed information on technique and inputs used for this measurement. Sections VIII and IX present the obtained result and the evaluation of the systematic uncertainties.

## II. MEASUREMENT METHOD

This measurement exploits the large semileptonic sample corresponding to approximately  $250 \text{ pb}^{-1}$  of integrated luminosity, accumulated by DØ during period from April 2002 to January 2004.  $B$  hadrons were selected using their semileptonic decays[3]  $B \rightarrow \mu^+ \nu \bar{D}^0 X$  and were classified into 2 exclusive groups: “ $D^*$ ” sample, containing all events with reconstructed  $D^{*-} \rightarrow \bar{D}^0 \pi^-$  decays, and “ $D^0$ ” sample, containing all remaining events. Both simulation and available experimental results show that the  $D^*$  sample is dominated by  $B_d^0 \rightarrow \mu^+ \nu D^{*-} X$  decays, while the  $\bar{D}^0$  sample is dominated by  $B^+ \rightarrow \mu^+ \nu \bar{D}^0 X$  decays.

Although the  $\mu^+ \nu \bar{D}^0 X$  selection depended on the  $B$ -hadron decay length, the classifications into 2 samples was done in a  $B$ -lifetime independent way. The only used criterion for this classification was the presence of an additional pion with correct charge and with the mass  $M(\bar{D}^0 \pi^-)$  close to the mass of  $D^{*-}$ . Construction of  $B$ -decay vertex and the measurement of  $B$ -hadron energy was done using  $\mu^+$  and  $\bar{D}^0$  in both samples, neglecting the information provided by the pion from  $D^*$  decay. In addition, special cuts were applied to obtain the same kinematic properties of particles in both samples.

Therefore, the decay length precision and the reconstruction efficiency were found to be essentially the same, and consequently the ratio of the number of events in 2 samples, expressed as a function of the proper decay length, depended mainly on the lifetime difference of  $B^+$  and  $B_d^0$  hadrons, while the influence on this ratio of the selection details or the detector properties was significantly reduced. The contribution of many systematic uncertainties, like the modeling of the semileptonic  $B$ -decays, should be also decreased. Thus, by directly measuring the difference of lifetimes of  $B^+$  and  $B_d^0$  using the ratio of events in 2 samples, a precise result can be obtained.

## III. DETECTOR DESCRIPTION

The DØ detector is comprised of the following main elements. A magnetic central tracking system, which consists of a silicon microstrip tracker (SMT) and a central fiber tracker (CFT), both located within a 2 Tesla superconducting solenoidal magnet [4]. The SMT has  $\sim 800,000$  individual strips, with typical pitch of 50-80  $\mu\text{m}$ , and a design optimized for tracking and vertexing capability up to  $|\eta| < 3$ . The system has a six-barrel longitudinal structure, each with a set of four layers arranged axially around the beam pipe, and interspersed with 16 radial disks. The CFT has eight thin coaxial barrels, each supporting two doublets of overlapping scintillating fibers of 0.835 mm diameter, one

doublet being parallel to the collision axis, and the other alternating by  $\pm 3^\circ$  relative to the axis. Light signals are transferred via clear light fibers to solid-state photon counters (VLPC) that have  $\approx 80\%$  quantum efficiency.

Central and forward preshower detectors located just outside of the superconducting coil (in front of the calorimetry) are constructed of several layers of extruded triangular scintillator strips that are read out using wavelength-shifting fibers and VLPCs. The next layer of detection involves three liquid-argon/uranium calorimeters: a central section (CC) covering  $|\eta| < 1$ , and two end calorimeters (EC) extending coverage to  $|\eta| < 4.0$ , all housed in separate cryostats [5]. In addition to the preshower detectors, scintillators between the CC and EC cryostats provide sampling of developing showers at  $1.1 < |\eta| < 1.4$ .

A muon system resides beyond the calorimetry, and consists of a layer of tracking detectors and scintillation trigger counters before 1.8 T toroids, followed by two more similar layers after the toroids. Tracking at  $|\eta| < 1$  relies on 10 cm wide drift tubes [5], while 1 cm mini-drift tubes are used at  $1 < |\eta| < 2$ .

The trigger and data acquisition systems are designed to accommodate the large luminosity of Run-II. Based on preliminary information from tracking, calorimetry, and muon systems, the output of the first level of the trigger is used to limit the rate for accepted events to  $\approx 1.5$  kHz. At the next trigger stage, with more refined information, the rate is reduced further to  $\approx 800$  Hz. These first two levels of triggering rely purely on hardware and firmware. The third and final level of the trigger, with access to all the event information, uses software algorithms and a computing farm, and reduces the output rate to  $\approx 50$  Hz, which is written to tape.

#### IV. EVENT SELECTION

Events were reconstructed using the standard version of DØ software. Muons were identified by the standard DØ tools and in addition were required to have a reconstructed track segment in at least one chamber outside the toroid, to have associated track in the central tracking system with both hits in SMT and CFT present, and to have the transverse momentum  $p_T^\mu > 2$  GeV/c, the pseudo-rapidity  $|\eta^\mu| < 2$  and the total momentum  $p^\mu > 3$  GeV/c.

All charged particles in event were clustered into jets using the DURHAM clustering algorithm [7] with the  $P_t$  cut-off parameter 15 GeV/c [8]. Events with more than one identified muon in the same jet were rejected, as well as the events with identified  $J/\psi \rightarrow \mu^+\mu^-$  decay.

The primary vertex of  $p\bar{p}$  interaction was determined in each event, using the method described in [9]. The crossing point of 2 beams, which has the resolution of about 30  $\mu\text{m}$ , was used as the constraint in the primary vertex fit. In average, 25 tracks were included in the primary vertex. The precision of the primary vertex reconstruction depended on the number of used tracks and was in average about 20  $\mu\text{m}$  in the plane perpendicular to the beam direction and about 45  $\mu\text{m}$  along the beam.

The  $\bar{D}^0$  candidate was constructed from two particles of the opposite charge belonging to the same jet as the reconstructed muon. Both particles were required to have hits in SMT and CFT, transverse momentum  $p_T > 0.7$  GeV/c and pseudo-rapidity  $|\eta| < 2$ . They were required to form a common  $D$ -vertex with the fit  $\chi_D^2 < 9$  per 1 degree of freedom. For each particle, the axial[10]  $\epsilon_T$  and stereo[11]  $\epsilon_L$  projections of the track impact parameter with respect to the primary vertex together with the corresponding errors ( $\sigma(\epsilon_T)$ ,  $\sigma(\epsilon_L)$ ) were computed. The combined significance  $(\epsilon_T/\sigma(\epsilon_T))^2 + (\epsilon_L/\sigma(\epsilon_L))^2$  was required to be greater than 4. The distance  $d_T^D$  between the primary and  $D$  vertices in the axial plane was required to exceed 4 standard deviations:  $d_T^D/\sigma(d_T^D) > 4$ . The angle  $\alpha_T^D$  between the  $\bar{D}^0$  momentum and the direction from the primary to the  $\bar{D}^0$  vertex in the axial plane was required to satisfy the condition:  $\cos(\alpha_T^D) > 0.9$ .

The tracks of muon and  $\bar{D}^0$  candidate were required to form a common  $B$ -vertex with fit  $\chi_B^2 < 9$  per 1 degree of freedom. The momentum of the  $B$  candidate was computed as the sum of the momenta of the  $\mu$  and  $\bar{D}^0$ . The mass of the  $(\mu^+\bar{D}^0)$  system was required to fall within  $2.3 < M(\mu^+\bar{D}^0) < 5.2$  GeV/c<sup>2</sup>. If the distance  $d_T^B$  between the primary and  $B$  vertices in the axial plane exceeded  $4 \cdot \sigma(d_T^B)$ , the angle  $\alpha_T^B$  between the  $B$  momentum and the direction from the primary to the  $B$  vertex in the axial plane was demanded to satisfy the condition:  $\cos(\alpha_T^B) > 0.95$ . The distance  $d_T^B$  was allowed to be greater than  $d_T^D$ , provided that the distance between the B and D vertices  $d_T^{BD}$  was less than  $3 \cdot \sigma(d_T^{BD})$ .

The mass spectrum of  $(K\pi)$  system after all these selections is shown in Fig.1. The masses of kaon and pion were assigned to the particles according to the charge of the muon, requiring the  $\mu^+K^+\pi^-$  final system or its charge conjugate. The mass spectrum with the opposite mass assignment  $\mu^+K^-\pi^+$ , also shown in Fig.1, does not give any mass structure, which confirms the correlated production of  $\mu^+\bar{D}^0$  system, as it is expected in  $B$  decay. The signal in the  $\bar{D}^0$  peak contains  $\sim 109000$  events.

Additional cuts, specific for this analysis, were further applied to this sample. They are discussed in the following sections.

For each  $\mu^+\bar{D}^0$  candidate, the additional pion with the charge opposite to the charge of muon was searched for. The mass difference  $\Delta M = M(\bar{D}^0\pi) - M(\bar{D}^0)$  for all such pions, when  $1.80 < M(\bar{D}^0) < 1.9$  GeV/c<sup>2</sup>, is shown in

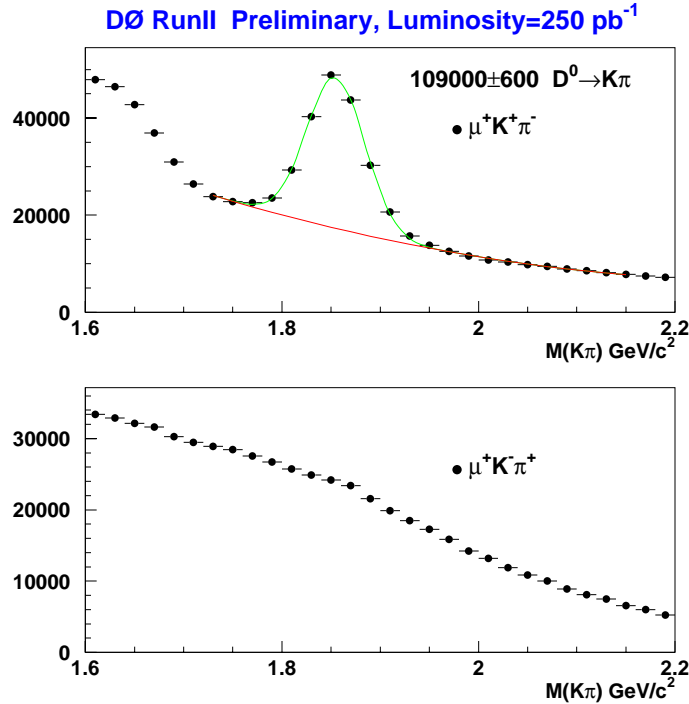


FIG. 1: The invariant mass of  $K\pi$  system for  $\mu^+K^+\pi^-$  (points with errors) and  $\mu^+K^-\pi^+$  (filled histogram) mass assignment. The curve shows the result of the fit of the  $K^+\pi^-$  mass distribution with Gaussian and polynomial background. Points in the left peak, corresponding to partially reconstructed decay  $\bar{D} \rightarrow K^+\pi^-X$ , were assigned a zero weight in this fit.

Fig.2. The peak, corresponding to the production of  $\mu^+D^{*-}$  system is clearly seen. All events containing the pion with the opposite to the muon charge (right charge combination) and giving  $0.1425 < \Delta M < 0.149$  GeV/c<sup>2</sup> were included into the  $D^{*R}$  sample.

The events containing a pion with the same charge as the muon give an estimate of the combinatorial background in the  $D^{*R}$  sample. The  $\Delta M$  distribution for such events is shown in Fig.2 as the filled histogram. All events containing the pion with the same as the muon charge (wrong charge combination) and giving  $0.1425 < \Delta M < 0.149$  GeV/c<sup>2</sup> were included into the auxiliary  $D^{*W}$  sample. All remaining events were assigned to the  $D^0$  sample.

The important feature of this analysis is that no any other criteria was applied to classify events into these samples. The simple fact of the presence of the pion in the event is sufficient to obtain a pure  $D^*$  signal. The estimated composition of selected samples is given in section VII A.

## V. EXPERIMENTAL OBSERVABLES $r_i$

The transverse decay length of a  $B$ -hadron  $L_T$  was defined as the distance in the axial plane between the primary vertex and vertex produced by the muon and  $\bar{D}^0$ . The transverse momentum of a  $B$ -hadron  $P_T^{\mu D^0}$  was defined as the vector sum of transverse momenta of muon and  $\bar{D}^0$ . The sign of the decay length was set positive, if the angle  $\alpha_T^B$ , defined in section IV, was less than  $\pi/2$ , otherwise it was set negative. The measured *visible proper decay length* (VPDL) was defined as:

$$x^M = L_T / P_T^{\mu D^0} \cdot M_B \quad (1)$$

Events in all samples were divided into 8 groups according to the measured VPDL, which are defined in Table I. The number of  $\mu^+\bar{D}^0$  events  $N_i^{*R}$  (from  $D^{*R}$  sample),  $N_i^{*W}$  (from  $D^{*W}$  sample) and  $N_i^0$  (from  $D^0$  sample) in each interval  $i$  were determined from the fit of the  $(K\pi)$  mass spectrum with the sum of a Gaussian and a polynomial background. The mean of the Gaussian was free parameter, while its R.M.S. was fixed to the value, obtained from the fit of the overall mass distribution in each sample. The result of the fit for on of intervals is shown in Fig.3.

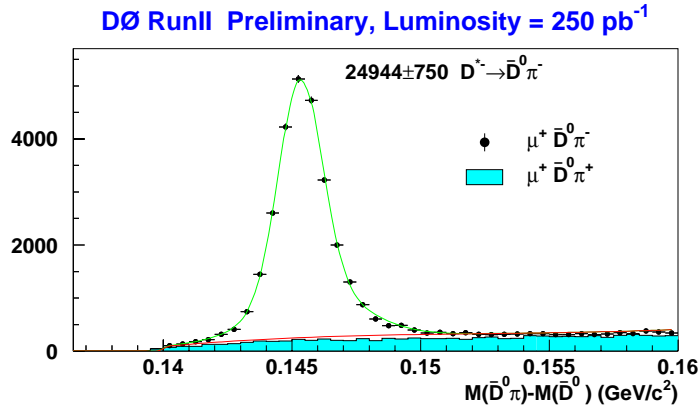


FIG. 2: The mass difference  $M(D^0\pi) - M(D^0)$  for events with  $1.80 < M(D^0) < 1.9$  GeV/ $c^2$ .

The  $D^{*R}$  sample contains mainly  $\mu^+ D^{*-}$  events, but also has a small contribution from  $\mu^+ \bar{D}^0$  events because this sample was defined by the window in the mass difference  $0.1425 < M(D^0\pi) - M(D^0) < 0.149$  GeV/ $c^2$  and included a combinatorial background under the  $D^*$  signal, see Fig. 2. This background was estimated using the  $D^{*W}$  sample, so that the number of  $\mu^+ D^{*-}$  events for each interval  $i$  in VPDL was defined as:

$$N_i(\mu^+ D^{*-}) = N_i^{*R} - C \cdot N_i^{*W} \quad (2)$$

The coefficient  $C = 1.22 \pm 0.04$  reflects the difference in the combinatorial background between the right and wrong charge combinations. It was taken as the ratio of events with right and wrong charge combinations with  $0.153 < \Delta M < 0.160$  GeV/ $c^2$ .

The  $D^{*W}$  sample contains genuine  $\mu^+ \bar{D}^0$  events with randomly associated pion. As it was explained above,  $D^{*R}$  sample also contains the small contribution from  $\mu^+ \bar{D}^0$  events, their number was estimated as  $C \cdot N_i^{*W}$ . Therefore, the number of  $\mu^+ \bar{D}^0$  events in each interval  $i$  in VPDL was defined as:

$$N_i(\mu^+ \bar{D}^0) = N_i^0 + N_i^{*W} + C \cdot N_i^{*W}. \quad (3)$$

The experimental observables  $r_i$  for this measurement, which represent the ratio of  $\mu D^*$  and  $\mu D^0$  events, were defined as:

$$r_i = \frac{N_i(\mu^+ D^{*-})}{N_i(\mu^+ \bar{D}^0)} = \frac{N_i^{*R} - C \cdot N_i^{*W}}{N_i^0 + (1 + C) \cdot N_i^{*W}}. \quad (4)$$

The definition of the decay length, transverse momentum and visible proper decay length was the same for both  $D^*$  and  $D^0$  samples. The numbers  $N_i^{*R}$ ,  $N_i^{*W}$  and  $N_i^0$  for all VPDL intervals were obtained from the  $(K\pi)$  mass spectrum using the same procedure, which significantly reduces the systematic uncertainties in  $r_i$ .

In addition to the selections of section IV, the cut  $\sigma(x^M) < 200$   $\mu\text{m}$  on the estimated precision of  $x^M$  was applied, to reduce the deformation of  $r_i$  by events with bad measurement of the VPDL. It should be compared with the average precision of the  $x^M \sim 35$   $\mu\text{m}$ . About 5% of events were removed by this cut.

## VI. EXPECTED VALUES $r_i^e$

For given decay channel  $j$  of  $B$ -hadron decay, the distribution of the visible proper decay length  $x$  is given by:

$$P_j(x) = \int dK Z_j(K) \cdot \theta(x) \cdot \frac{K}{c\tau_j} \exp\left(-\frac{Kx}{c\tau_j}\right); \quad K = P_T^{\mu D^0} / P_T^B. \quad (5)$$

Here  $\tau_j$  is the lifetime of  $B$ -hadron,  $K$ -factor reflects the difference between the observed and true momenta of  $B$ -hadron,  $\theta(x)$  takes into account that only positive values of  $x$  are possible. The function  $Z_j(K)$  gives the normalised distribution of the  $K$ -factor in a given channel  $j$ .

TABLE I: Definition of 8 intervals in VPDL, For each interval  $i$  the number of events in  $D^{*R}$ ,  $D^{*W}$  and  $D^0$  samples, the ratio  $r_i$  and the expected value  $r_i^e$  for  $\tau^+/\tau^0 - 1 = 0.093$  are given.

$i$	VPDL range(cm)	$N_i^{*R}$	$N_i^{*W}$	$N_i^0 + N_i^{*W}$	$r_i$	$r_i^e$
1	[-0.1,0.0]	1016 ± 39	43 ± 18	3175 ± 109	0.298±0.018	0.325
2	[0.0,0.02]	3482 ± 69	129 ± 22	9973 ± 162	0.328±0.009	0.324
3	[0.02,0.04]	3350 ± 67	111 ± 18	9850 ± 152	0.322±0.009	0.318
4	[0.04,0.07]	3593 ± 70	114 ± 18	10995 ± 155	0.310±0.008	0.310
5	[0.07,0.10]	2175 ± 55	75 ± 13	7144 ± 126	0.288±0.010	0.301
6	[0.10,0.15]	1932 ± 51	57 ± 13	6349 ± 120	0.290±0.010	0.291
7	[0.15,0.25]	1212 ± 42	36 ± 11	4189 ± 102	0.276±0.013	0.274
8	[0.25,0.40]	298 ± 21	5 ± 6	1022 ± 51	0.284±0.027	0.252

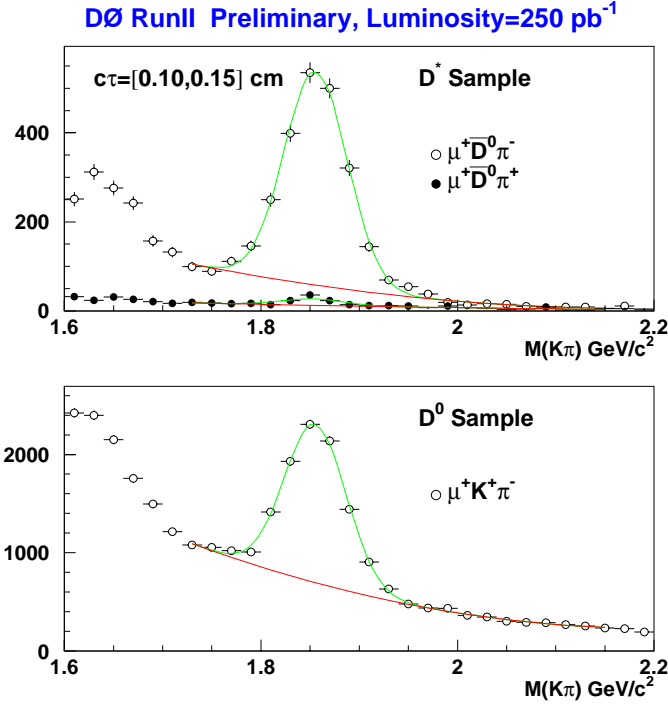


FIG. 3: The  $K\pi$  mass distribution for events with VPDL between 0.10 and 0.15 cm in  $D^{*R}$  (open circles in the upper plot),  $D^{*W}$  (filled circles in the upper plot) and  $D^0$  (lower plot) samples. The curves show the result of the fit of the mass distribution between 1.72 and 2.16  $\text{GeV}/c^2$  with the Gaussian and polynomial background.

Transformation from the true  $x$  to the experimentally measured value  $x^M$  is given by:

$$f_j(x^M) = \int dx \text{Res}_j(x - x^M) \cdot \text{Eff}_j(x) \cdot P_j(x). \quad (6)$$

Here  $\text{Res}_j(x - x^M)$  is the detector resolution of the VPDL and  $\text{Eff}_j(x)$  is the reconstruction efficiency of given channel  $j$ .

Finally, the expected value  $r_i^e$  for a given interval  $i$  of the measured VPDL is given by:

$$r_i^e = \frac{F_i^*}{F_i^0}; \quad F_i^{*,0} = \int_i dx^M \sum_j Br_j \cdot f_j(x^M). \quad (7)$$

Here the integration  $\int_i dx^M$  is taken over the given interval  $i$ , the  $\sum_j$  is taken over all decay channels  $B \rightarrow \mu^+ \nu D^{*-} X$  and  $B \rightarrow \mu^+ \nu \bar{D}^0 X$  for  $F_i^*$  and  $F_i^0$  respectively, and the  $Br_j$  is the branching rate of given channel  $j$ .

The measure of lifetime difference between  $B_d^0$  and  $B^+$  is given by  $k \equiv \tau^+/\tau^0 - 1$ . It was determined from the minimization of  $\chi^2(N, k)$ :

$$\chi^2(N, k) = \sum_i \frac{(r_i - N \cdot r_i^e(k))^2}{\sigma^2(r_i)}, \quad (8)$$

where  $N$  stands for the global normalisation coefficient, which, along with  $k$ , was a free parameter in the minimization. It absorbed many uncertainties coming from the modeling of background in  $D^0$  fit, reconstruction efficiencies etc. The  $\sum_i$  was taken over all intervals with positive VPD. The interval with negative VPD was used for the control of resolution difference in  $D^*$  and  $D^0$  samples, see section VII C.

For the computation of  $r_i^e$ , the  $B^+$  lifetime  $\tau^+ = 1.674 \pm 0.018$  was taken from the PDG and  $B_d^0$  lifetime  $\tau^0$  was expressed as  $\tau^0 = \tau^+/(1+k)$ , the  $Br_j$  were taken from the PDG and the  $Z_j(K)$ ,  $Res_j(x)$  and  $Eff_j(x)$  were taken from the simulation. All these inputs, discussed in the following section, contribute to the systematic uncertainties. However, most of them cancel in the ratios  $r_i^e$ , so that a precise measurement of the lifetime difference can be obtained.

## VII. INPUTS TO $r_i^e$

### A. Decay Channels and Branching Rates

To determine the composition of selected samples, the following decay channels of B mesons were considered for  $D^*$  sample:

$$B_d^0 \rightarrow \mu^+ \nu D^{*-}; B_d^0 \rightarrow \mu^+ \nu D^{**} \rightarrow \mu^+ \nu D^{*-} X; B^+ \rightarrow \mu^+ \nu \bar{D}^{*0} \rightarrow \mu^+ \nu D^{*-} X; B_s^0 \rightarrow \mu^+ \nu D^{*-} X.$$

The following decay channels were considered for  $D^0$  sample:

$$B^+ \rightarrow \mu^+ \nu \bar{D}^0; B^+ \rightarrow \mu^+ \nu \bar{D}^{*0}; B^+ \rightarrow \mu^+ \nu \bar{D}^{**0} \rightarrow \mu^+ \nu \bar{D}^0 X; B^+ \rightarrow \mu^+ \nu \bar{D}^{**0} \rightarrow \mu^+ \nu \bar{D}^{*0} X;$$

$$B_s^0 \rightarrow \mu^+ \nu \bar{D}^0 X; B_s^0 \rightarrow \mu^+ \nu \bar{D}^{*0} X; B_d^0 \rightarrow \mu^+ \nu D^{**} \rightarrow \mu^+ \nu \bar{D}^0 X; B_d^0 \rightarrow \mu^+ \nu D^{**} \rightarrow \mu^+ \nu \bar{D}^{*0} X.$$

Here and in the following the symbol “ $D^{**}$ ” denotes both narrow and wide  $D^{**}$  resonances, together with non-resonant  $D X$  and  $D^* X$  production.

The latest PDG values[6] were used to determine the branching fractions of decays contributing to the  $D^0$  and  $D^*$  samples:

$$\begin{aligned} Br(B^+ \rightarrow \mu^+ \nu \bar{D}^0) &= 2.15 \pm 0.22\%; & Br(B^0 \rightarrow \mu^+ \nu D^-) &= 2.14 \pm 0.20\%; \\ Br(B^+ \rightarrow \mu^+ \nu \bar{D}^{*0}) &= 6.5 \pm 0.5\%; & Br(B^0 \rightarrow \mu^+ \nu D^{*-}) &= 5.53 \pm 0.23\%. \end{aligned}$$

The  $Br(B^+ \rightarrow \mu^+ \nu \bar{D}^{**0})$  was estimated using the following inputs:

$$\begin{aligned} Br(B^0 \rightarrow \mu^+ \nu D^{**}) &= \tau^0/\tau^+ \cdot Br(B^+ \rightarrow \mu^+ \nu \bar{D}^{**0}); \\ Br(B \rightarrow \mu^+ \nu \bar{D}^{**}) &= Br(B \rightarrow \mu^+ \nu X) - Br(B \rightarrow \mu^+ \nu \bar{D}) - Br(B \rightarrow \mu^+ \nu \bar{D}^*); \\ Br(B \rightarrow l^+ \nu X) &= 10.7 \pm 0.28\% \text{ (PDG)}; \end{aligned}$$

The measurement of ARGUS [12]  $Br(B \rightarrow \mu^+ \nu \bar{D}^{**}) = 2.7 \pm 0.7\%$ , although included in averaging procedures of HFAG, is not used here, since it is model dependent. From these numbers we obtained:

$$Br(B^+ \rightarrow \mu^+ \nu \bar{D}^{**0}) = 2.67 \pm 0.37\% \quad (9)$$

The  $Br(B^+ \rightarrow \mu^+ \nu \bar{D}^{**0} \rightarrow \mu^+ \nu D^{*-} X)$  was estimated from the following measurements:

$$\begin{aligned} Br(\bar{b} \rightarrow l^+ \nu D^{*-} \pi^+ X) &= (4.73 \pm 0.77 \pm 0.55) \cdot 10^{-3} \text{ (ALEPH [13])}; \\ Br(\bar{b} \rightarrow l^+ \nu D^{*-} \pi^+ X) &= (4.80 \pm 0.9 \pm 0.5) \cdot 10^{-3} \text{ (DELPHI [14])}; \\ Br(\bar{b} \rightarrow l^+ \nu D^{*-} \pi^- X) &= (0.6 \pm 0.7 \pm 0.2) \cdot 10^{-3} \text{ (DELPHI [14])}; \\ Br(b \rightarrow B^+) &= Br(b \rightarrow B^0) = 0.389 \pm 0.013, \text{ (PDG [6])}. \end{aligned}$$

The usual practice in estimating this decay rate is to neglect the contribution of  $D^{**} \rightarrow D^* \pi \pi$ , see e.g. [15]. However, listed above data allow to take into account these decays also. Neglecting  $D^{**} \rightarrow D^* \pi \pi$ , which give  $\sim 1\%$  contribution to  $D^{**}$  decays according to simulation, the available measurements can be expressed as:

$$\begin{aligned} Br(\bar{B} \rightarrow l^+ \nu D^{*-} \pi^+ X) &= Br(B^+ \rightarrow l^+ \nu D^{*-} \pi^+ X^0) + Br(B^0 \rightarrow l^+ \nu D^{*-} \pi^+ \pi^-) \\ Br(\bar{B} \rightarrow l^+ \nu D^{*-} \pi^- X) &= Br(B^0 \rightarrow l^+ \nu D^{*-} \pi^+ \pi^-) \end{aligned}$$

From these relations and using listed above measurements, we obtain:

$$Br(B^+ \rightarrow \mu^+ \nu \bar{D}^{**0} \rightarrow l^+ \nu D^{*-} X) = 1.07 \pm 0.25\% \quad (10)$$

All other rates  $Br(B \rightarrow \mu^+ \nu \bar{D}^{**} \rightarrow \mu^+ \nu \bar{D}^* X)$  were obtained using the following relations:

$$Br(B^0 \rightarrow \mu^+ \nu D^{**} \rightarrow \mu^+ \nu D^* X) = \tau^0/\tau^+ \cdot Br(B^+ \rightarrow \mu^+ \nu \bar{D}^{**0} \rightarrow \mu^+ \nu D^* X);$$

$Br(B^+ \rightarrow \mu^+ \nu \bar{D}^{*0} \rightarrow \mu^+ \nu D^{*-} X^+) = 2 \cdot Br(B^+ \rightarrow \mu^+ \nu \bar{D}^{*0} \rightarrow \mu^+ \nu \bar{D}^{*0} X^0)$  (isospin invariance);

$Br(B^0 \rightarrow \mu^+ \nu D^{*-} \rightarrow \mu^+ \nu \bar{D}^{*0} X^-) = 2 \cdot Br(B^0 \rightarrow \mu^+ \nu D^{*-} \rightarrow D^{*-} X^0)$  (isospin invariance);

Here  $X^+$ ,  $X^-$ ,  $X^0$  stand for one or many pions with total charge +1, -1 or 0.

The following inputs were used for the estimate of  $Br(B \rightarrow \mu^+ \nu \bar{D}^{*0} \rightarrow \mu^+ \nu \bar{D} X)$ :

$Br(B^+ \rightarrow \mu^+ \nu \bar{D}^{*0} \rightarrow \mu^+ \nu D^- X^+) = 2 \cdot Br(B^+ \rightarrow \mu^+ \nu \bar{D}^{*0} \rightarrow \mu^+ \nu \bar{D}^0 X^0)$  (isospin invariance);

$Br(B^0 \rightarrow \mu^+ \nu D^{*-} \rightarrow \mu^+ \nu \bar{D}^0 X^-) = 2 \cdot Br(B^0 \rightarrow \mu^+ \nu D^{*-} \rightarrow D^- X^0)$  (isospin invariance);

$Br(B \rightarrow \mu^+ \nu \bar{D}^{*0} \rightarrow \mu^+ \nu \bar{D} X) = Br(B \rightarrow \mu^+ \nu \bar{D}^{*0}) - Br(B \rightarrow \mu^+ \nu \bar{D}^{*0} \rightarrow \mu^+ \nu \bar{D}^* X)$ .

The following inputs were used for the estimate of  $B_s^0$  branching rates:

$Br(B_s^0 \rightarrow \mu^+ \nu X) = \tau^s / \tau^d \cdot Br(B_d^0 \rightarrow \mu^+ \nu X)$ ;

$Br(B_s^0 \rightarrow \mu^+ \nu D_s^- X) = 7.9 \pm 2.4\%$ [6];

$Br(B_s^0 \rightarrow \mu^+ \nu D_s^{*-} \rightarrow \mu^+ \nu \bar{D}^{*0} X) = Br(B_s^0 \rightarrow \mu^+ \nu D_s^{*-} \rightarrow \mu^+ \nu \bar{D}^{*0} X)$  (isospin invariance).

In addition, it was supposed, that:

$$R_s^{**} = \frac{Br(B_s^0 \rightarrow \mu^+ \nu D_s^{*-} \rightarrow \mu^+ \nu D^* X)}{Br(B_s^0 \rightarrow \mu^+ \nu D_s^{**})} = 0.35 \quad (11)$$

There is no experimental measurement of this rate yet and for the estimate of the contribution to the systematics this rate varied between 0 and 1.

According to the above information, the  $D^*$  sample contains a 85% of  $B_d^0$  and 15% of  $B^+$  decays. The  $D^0$  sample correspondingly has a 85% contribution from  $B^0$  and 15% contribution from  $B^+$ . These numbers do not take into account the reconstruction efficiencies in different channels and  $B_s^0$  contribution. The sample composition can also be extracted from the MC simulation. The decay rates used for the DØ generation of  $B$ -hadron decays give 87% contribution from  $B^+$  and 13% contribution from  $B^0$  in the  $D^*$  sample. The  $D^0$  sample has a 83% contribution from  $B^0$  and 17% contribution from  $B^+$ . These numbers are in a very good agreement with the experimental measurements. Taking into account the reconstruction efficiencies (see sec.VII C) and  $B_s^0$  contribution,  $D^*$  sample contains 86%  $B_d^0$ , 12%  $B^+$  and 2%  $B_s^0$ , while  $D^0$  sample contains 82%  $B^+$ , 16%  $B_d^0$  and 2%  $B_s^0$ .

## B. $K$ -factors

Semileptonic  $B$  decays necessarily have a neutrino present in the decay chain making impossible a precise determination of the kinematics for the  $B$  meson. This leads to a bias towards smaller values of the momentum of  $B$ , calculated using the registered particles only. A common practice to correct this bias is to scale the measured momentum of  $B$  by a  $K$ -factor, which takes into account the effect of neutrino. The  $K$ -factor was estimated from the simulation. For this analysis it was defined as:

$$K = p_T(\mu D^0) / p_T(B), \quad (12)$$

where  $p_T$  denotes the absolute value of transverse momentum. The slow pion from  $D^{*-}$  decay was not included in  $p_T(\mu D^0)$ , which made the  $K$ -factors for  $B \rightarrow D^{*-} X$  and  $B \rightarrow \bar{D}^{*0} X$  very similar, since  $\pi^0/\gamma$  from  $\bar{D}^{*0}$  decay was not reconstructed as well. The  $D^*$  production dominates both for  $B^+$  and  $B^0$  decays, see section VII A, therefore defining  $K$ -factors to be similar for  $D^{*-}$  and  $\bar{D}^{*0}$  should help to cancel out the uncertainties of the  $K$ -factor modeling in the lifetime ratio measurement.

Following the definition (12), the  $K$ -factors for all considered decays were combined into five groups:  $B \rightarrow \mu^+ \nu \bar{D}^* X$ ;  $B \rightarrow \mu^+ \nu \bar{D}^0 X$ ;  $B \rightarrow \mu^+ \nu \bar{D}^{*0} X \rightarrow \mu^+ \nu \bar{D}^* X$ ;  $B \rightarrow \mu^+ \nu \bar{D}^{*0} X \rightarrow \mu^+ \nu \bar{D}^0 X$ ;  $B_s \rightarrow \mu^+ \nu \bar{D}^0 X$ . The  $K$ -factor distributions  $Z_j(K)$  were determined separately for each group and were used for the computation of expected values  $r_i$ , see 5.

## C. Reconstruction Efficiencies and Resolution

The efficiency to reconstruct  $\mu^+ D^0$  final state in a process  $B \rightarrow Y$  was expressed as:

$$Eff(x; B \rightarrow Y) = C_Y \cdot Eff(x; B^+ \rightarrow \mu^+ \nu \bar{D}^{*0}) \quad (13)$$

The deviation of coefficients  $C_Y$  from unity arises only due to differences in kinematics of considered processes and does not change with the lifetime. Numerically,  $C_Y$  vary between 1.26 and 0.73, depending on the process. The efficiency to reconstruct  $B^+ \rightarrow \mu^+ \nu \bar{D}^{*0}$  and coefficients  $C_Y$  were taken from the simulation, the influence of uncertainty in their values on the final result is discussed in section IX.

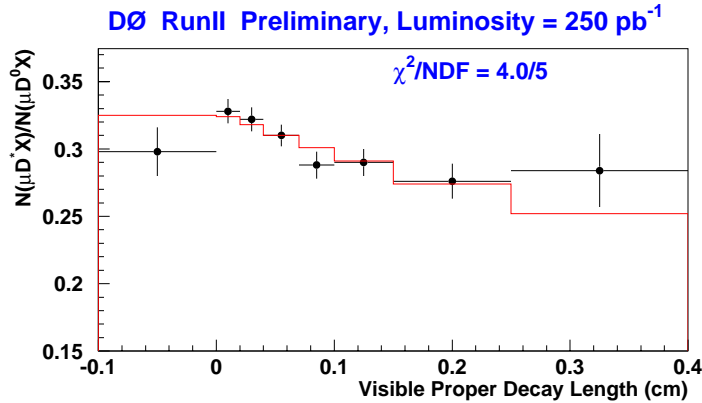


FIG. 4: The ratio of events in  $D^*$  and  $D^0$  samples as a function of the visible proper decay length. The result of the minimization of (8) with  $k = 0.093$  is shown as a histogram.

Additionally, for all channels with reconstructed  $D^{*+}$ , the efficiency  $Eff(x; \pi)$  to select pion from decay  $D^{*+} \rightarrow D^0 \pi^+$  should be taken into account:

$$Eff(x; D^*) = Eff(x; \pi) \cdot Eff(x; D^0) \quad (14)$$

The selection of  $D^*$  was explicitly constructed in a way to exclude any direct dependence of the  $Eff(x; \pi)$  on the lifetime. Still, the reconstruction of the slow pion depends on the  $D^0$  momentum, because of the software cut on the minimal transverse momentum of reconstructed tracks  $p_T > 0.183$  GeV/c. This dependence, although not directly related with the decay length, could induce the second order correlation of the efficiency and the VPDL. Both data and simulation show that the variation of  $Eff(x; \pi)$  is significant below  $p_T(D^0) = 5$  GeV/c and becomes reasonably flat above this threshold. Therefore, to remove any possible lifetime dependence in the  $Eff(x; \pi)$ , the additional cut  $p_T(D^0) > 5$  GeV/c was applied to the selected events.

Although this cut reduces the sample by  $\sim 35\%$ , it ensures the validity of  $Eff(x; \pi)$  and considerably reduces the corresponding systematics. In addition, it helps to reduce the background contributions from  $B \rightarrow \bar{D} D_s X$  and  $c\bar{c}$  productions. After this cut, the  $Eff(x; \pi) \simeq 0.88$  in the simulation and does not depend on the proper decay length within the simulation statistical errors. This value was used to extract the lifetime ratio. The systematic uncertainties from this source are discussed in section IX.

For this measurement the VPDL resolution was taken from the simulation and was assumed to be the same for  $D^*$  and  $D^0$  samples, since exactly the same procedure was used to measure the decay length in all samples. The influence of possible differences in resolution description between data and simulation on the lifetime ratio is discussed in the section IX.

## VIII. RESULTS

As explained previously, two additional cuts were applied to the sample selected in section IV. The expected precision of the visible proper decay length was required to be less than  $200 \mu\text{m}$  and the transverse momentum of the  $\bar{D}^0$  should be more than  $5$  GeV/c. With these selections  $69870 \mu^+ \bar{D}^0$  events were selected. The obtained values of  $r_i$  together with their errors are given in Table I. Minimization of the  $\chi^2$  distribution (8) gives:

$$k \equiv \frac{\tau^+}{\tau^0} - 1 = 0.093 \pm 0.021 \text{ (stat)} \quad (15)$$

$$N = 1.001 \pm 0.012$$

The value of  $\chi^2/NDF$  in the minimum is  $4.0/5$ . Fig.4 present the  $r_i$  values together with the result of the fit.

## IX. SYSTEMATIC ERRORS AND CONSISTENCY CHECKS

The influence of various source of systematics on the final result is summarized in Table II. Different contributions can be divided into 3 groups. The first part includes uncertainties coming from the errors of the experimental measurements, like the branching rates, lifetimes etc. All inputs were varied by one standard deviation, only contribution exceeding 0.0001 in the error on  $k$  are listed in Table II. The uncertainty in  $Br(B^+ \rightarrow \mu^+ \nu \bar{D}^{*0} \rightarrow \mu^+ \nu D^{*-} X)$  gives the maximal impact on the result.

The second group includes uncertainties coming from the inputs taken from the simulation. The uncertainty from the VPDL-dependent efficiency to reconstruct  $B^+ \rightarrow \mu^+ \nu \bar{D}^{*0}$  was estimated by repeating analysis with this efficiency set to a constant.

The variable  $N$  strongly depends on the efficiency  $Eff(x; \pi)$  and on the different branching rates, like  $Br(B_d^0 \rightarrow \mu^+ \nu D^{*-})$ . The value of  $N$ , obtained from the fit, is close to one, which indicates good agreement of  $Eff(x; \pi)$  in data and in simulation. Changing experimental branching rates within their statistical errors and keeping  $N$  equal to 1 results in the variation of the efficiency  $Eff(x; \pi)$  by  $\pm 0.04$ . This value was used to estimate the uncertainty in the lifetime rate.

The deviation of  $Eff(x; \pi)$  from the constant value can influence the result. The simulation does not show any indication of this deviation after the cut  $P_t(D^0) > 5$  GeV/c. The possible slope in  $Eff(x; \pi)$ , parametrized by the straight line, is  $-0.014 \pm 0.06$  [1/cm], where the error is determined by the limited simulation statistics. To estimate the systematic error from the uncertainty in the slope, it was varied by twice the value of its error:  $\pm 0.12$  [1/cm]. This uncertainty produces the largest systematic error in  $\tau^+/\tau^0$  measurement, it can be improved later with a better estimate.

As discussed in section VII C, the coefficients  $C_Y$  depend only on the kinematic properties of corresponding decays and can therefore be reliably estimated in the simulation. The corresponding uncertainty was estimated by setting all values  $C_Y$  to one.

The VPDL resolution, obtained in simulation, was multiplied by large factor, from 0.2 to 4.0, which significantly exceeds the estimated difference in resolution between data and simulation.

The difference in resolution between  $D^*$  and  $D^0$  samples could influence the measurement of the lifetime ratio, and the estimate of systematics due to this effect was obtained from the comparison of expected and measured values of  $r_1$  for events with negative VPDL, see Table I. The observed difference in  $r_1$ , which is about 1.5 standard deviation, can be the statistical fluctuation. Nevertheless, supposing that the difference in  $r_1$  is caused by differences in the VPDL resolution and increasing the fraction of events with bad VPDL resolution in  $D^0$  sample, described by the gaussian with the largest R.M.S. = 131  $\mu\text{m}$ , the exact agreement in the  $r_1$  value can be obtained. The corresponding change in the lifetime ratio was taken as the estimate of the systematic error from this source. This estimate did not change with the variation of the R.M.S. up to 3000  $\mu\text{m}$ .

The variation of  $K$ -factors with the change of  $B$  momentum was neglected in this analysis. To check the impact of this assumption on the final result, their computation was repeated without cut on  $p_t(D^0)$  or by applying additional cut 4 GeV/c on  $p_t$  of muon. The change of average value of  $K$ -factors did not exceed 2%, which was used as the estimate of the systematic uncertainty in their values.

Distributions of  $K$ -factors were used separately for decays  $B \rightarrow \mu^+ \nu \bar{D}^0$ ,  $B \rightarrow \mu^+ \nu \bar{D}^{*0}$ ,  $B \rightarrow \mu^+ \nu \bar{D}^{*0} \rightarrow \bar{D}^0 X$  and  $B \rightarrow \mu^+ \nu \bar{D}^{*0} \rightarrow \bar{D}^{*0} X$ . To take into account the uncertainty in the description of  $\bar{D}^{*0}$  decays, which are not well studied yet, the distributions of  $K$ -factors from  $B \rightarrow \bar{D}^{*0}$  decays were taken the same as for  $B \rightarrow \bar{D}^0(\bar{D}^{*0})$  decays.

One more source of systematics comes from the determination of the number of  $D^*$  and  $D^0$  events in each lifetime bin. As can be seen from figures 3, the signal is accompanied by significant background. Different parametrizations of the signal and background were tried. The maximal variation of the obtained result was taken as the systematic error from the background parametrization.

Finally, the uncertainty in coefficient  $C = 1.22 \pm 0.04$  from equation 2 gives a small contribution in the systematics, which was also taken into account.

All systematic uncertainties were added in quadrature and the total systematic error of the lifetime ratio  $\sigma(\tau^+/\tau^0) = 0.022$  was obtained. Many entries into the systematics can be considerably reduced after performing a more accurate study.

Different consistency tests of these measurements were tried. The total sample of events was divided in two parts using different criteria and the measurement was repeated independently in each sample. The definition of intervals was varied, one more VPDL interval between 0.4 and 0.8 cm was added or the last interval between 0.25 and 0.4 cm was removed from the fit. In all cases, the results are consistent within the statistical errors. Finally, the measurement of the lifetime ratio was performed with simulated events. The resulting value  $k^{MC} = 0.073 \pm 0.030$  agrees well with the generated lifetime ratio  $k^{gen} = 0.070$ .

TABLE II: Systematic uncertainties of the  $\tau^+/\tau^0$  measurement.

source	variation range	$\Delta(\tau^+/\tau^0)$
$Br(B_d^0 \rightarrow \mu^+ \nu D^{*-})$	$5.53 \pm 0.23\%$	0.0015
$Br(B^+ \rightarrow \mu^+ \nu \bar{D}^{*0})$	$6.50 \pm 0.5\%$	0.0001
$Br(B^+ \rightarrow \mu^+ \nu \bar{D}^{*0})$	$2.67 \pm 0.37\%$	0.0005
$Br(B^+ \rightarrow \mu^+ \nu D^{*-} \pi^+ X)$	$1.06 \pm 0.25\%$	0.0074
$Br(B_s^0 \rightarrow \mu^+ \nu D_s X)$	$7.9 \pm 2.4\%$	0.0025
$R_s^{**}$ , see (11)	$0 \div 1$	0.0007
$Eff(x; B^+ \rightarrow \mu^+ \nu D^{*0})$	set $Eff(x) = const$	0.0012
$Eff(\pi)$	$0.876 \pm 0.04$	0.0012
Time dependence of $Eff(x; \pi)$	slope $\pm 0.12$ [1/cm]	0.0132
$C_Y$	$C_Y = 1$	0.0086
VPDL resolution	MC resolution $\times (0.2 \div 4.0)$	0.0042
difference in resolution between $D^*$ and $D^0$	$r_1^e \rightarrow r_1$	0.0060
$K$ -factors	average value $\pm 2\%$	0.0021
$K$ -factors	$Z(K; D^{**}) = Z(K; D^0, D^*)$	0.0072
Fitting procedure	see section IX	0.0060
$C$ from eqn. (2)	$1.22 \pm 0.04$	0.0004
Total		0.0215

## X. CONCLUSIONS

The precise measurement of the lifetime difference between  $B^+$  and  $B^0$  mesons was performed. The large semileptonic sample corresponding to approximately  $250 \text{ pb}^{-1}$  of integrated luminosity, accumulated by DØ during period from April 2002 to January 2004, was analysed and about 70000 ( $\mu^+ D^0 X$ ) events were selected for the analysis. Using this record statistics, the preliminary lifetime difference between  $B^+$  and  $B^0$  mesons was found:

$$k = \frac{\tau^+}{\tau^0} - 1 = 0.093 \pm 0.021 \text{ (stat)} \pm 0.022 \text{ (syst)} \quad (16)$$

This result agrees well with the world average measurement  $k = 0.085 \pm 0.017$  and gives one of the most precise measurements of this parameter.

## Acknowledgments

We thank the staffs at Fermilab and collaborating institutions, and acknowledge support from the Department of Energy and National Science Foundation (USA), Commissariat à l'Énergie Atomique and CNRS/Institut National de Physique Nucléaire et de Physique des Particules (France), Ministry for Science and Technology and Ministry for Atomic Energy (Russia), CAPES, CNPq and FAPERJ (Brazil), Departments of Atomic Energy and Science and Education (India), Colciencias (Colombia), CONACyT (Mexico), Ministry of Education and KOSEF (Korea), CONICET and UBACyT (Argentina), The Foundation for Fundamental Research on Matter (The Netherlands), PPARC (United Kingdom), Ministry of Education (Czech Republic), A.P. Sloan Foundation, Civilian Research and Development Foundation, Research Corporation, Texas Advanced Research Program, and the Alexander von Humboldt Foundation.

- 
- [1] I.I. Bigi, hep-ph/0001003
  - [2] U.Nierste hep-ph/0209008
  - [3] Charge conjugated states are always implied in this paper.
  - [4] V.Abazov et al., in preparation for submission to Nucl. Instrum. Methods Phys. Res. A, and T. LeCompte and H.T.Diehl, Ann. Rev. Nucl. Part. Sci. **50**, 71 (2000).
  - [5] S. Abachi, *et al.*, Nucl. Instrum. Methods Phys. Res. A **338**, 185 (1994).
  - [6] K. Hagiwara et al, Phys. Rev. **D66**, 010001 (2002) and 2003 off-year partial update for the 2004 edition available on the PDG WWW pages (URL: <http://pdg.lbl.gov/>)
  - [7] S.Catani, Yu.L.Dokshitzer, M.Olsson, G.Turnock, B.R.Webber, Phys.Lett. **B269** (1991) 432.
  - [8] T.Sjöstrand et. al. hep-ph/0108264

- [9] DELPHI Collab., Eur.Phys.J. **C32** (2004) 185.
- [10] plane perpendicular to the beam direction.
- [11] parallel to the beam direction
- [12] H.Albrecht *et al.*, Zeit. Phys. **C57** (1993), 533.
- [13] D.Buskulic *et al.*, Zeit. Phys. **C73** (1997), 601-612.
- [14] P.Abreu *et al.*, Phys.Lett. **B475** (2000), 407.
- [15] D.Abbaneo *et al.* , “Combined results on b-hadron production rates and decay properties,” [arXiv:hep-ex/0112028](https://arxiv.org/abs/hep-ex/0112028).